

# Contribution of the eccentricity of unbonded tendons to the punching shear resistance of prestressed flat slabs

Elyson A. P. Liberati<sup>1</sup>, Heraldo Brigo<sup>1</sup>, Marília G. Marques<sup>2</sup>, Leandro M. Trautwein<sup>3</sup>

<sup>1</sup> Dept. of Civil Engineering, State University of Maringá  
Av. Colombo, n° 5790, 87020-900, Maringá/Paraná, Brazil  
[eapliberati@uem.br](mailto:eapliberati@uem.br), [hbrigo@gmail.com](mailto:hbrigo@gmail.com)

<sup>2</sup> Institute of Exact and Technological Sciences, Federal University of Viçosa  
Rodovia BR 230 KM 7, 38810-000, Rio Paranaíba /Minas Gerais, Brazil  
[marilia.marques@ufv.br](mailto:marilia.marques@ufv.br)

<sup>3</sup> School of Civil Engineering, University of Campinas, Campinas, São Paulo, Brazil  
R. Saturnino de Brito, 224, 13083-889, Campinas/São Paulo, Brazil  
[leandromt@fec.unicamp.br](mailto:leandromt@fec.unicamp.br)

**Abstract.** With the increasing use of prestressed flat slabs in floor construction, studies are needed to assess the high shear stresses generated in the slab-column connection, which is a vulnerable point to punching failure and crucial for the design of this constructive system. Together with experimental studies, the use of computational tools has allowed the analysis of the influence of prestressing on the ultimate resistance and thus the understanding of the puncture phenomenon through numerical simulations. In this study, experimental tests were simulated through nonlinear three-dimensional analysis using the computational program ATENA. The nonlinear behavior of cracked concrete and the yielding of steel in passive and active reinforcement was considered. The load-displacement and load-strain curves were compared between the experimental and numerical results obtained, with the aim of validating the constitutive models adopted for concrete and steel. From the adequate calibration of models, a parametric study was carried out with variations in the spacing and eccentricity of the tendons in the slab, thus allowing to identify the influence of these parameters on the punching shear resistance.

**Keywords:** punching shear, flat slabs, prestressed concrete, numerical analysis.

## 1 Introduction

The flat slab system has become an increasingly widespread constructive option, featuring slabs that rest rigidly and directly on the columns. Among its advantages are speed of execution, reduction of ceiling clearance, more economical foundations, and flexible layouts. As there are no beams in this structural system, the direct contact of the column with the slab provides high shear stresses, causing the punching phenomenon. According to Melges [1], this phenomenon can be basically defined as the perforation of a plate caused by forces acting in small areas, causing a brittle shear rupture in the connection between the slab and the column. According to Vecchio et al. [2] and Brigo et al. [3], this phenomenon can be caused due to its loading or its boundary conditions in different positions along the structure.

Among the alternatives for preventing this phenomenon in flat slabs, one can mention the use of shear reinforcement, increasing the rate of longitudinal bars, adding fibers to the concrete or the use of prestressed concrete. Several researchers such as Melges [1], Vecchio et al. [2], Nylander and Kinnunen [4], Pralong and Brändli [5], Shehata [6], Corrêa [7], Ramos et al. [8] and Clément et al. [9] revealed the beneficial effects caused by the application of prestressing on flat slabs in different ways of design, whether with straight or parabolic cables, with and without eccentricity or external prestressing.

With the introduction of prestressing, the normal compressive stresses in the slab plane are increased, which increases its bearing capacity, in addition to reducing concrete cracking and increasing punching shear resistance. Studies such as those by Clément et al. [9], Diaz et al. [10] and El-Sisi et al. [11] revealed the interference caused by the eccentricity of the prestressing strand layouts, which results in bending moments opposite to those of external actions. According to Clément et al. [9], since the vertical portions of the prestressing forces are intercepted by the drilling failure surface, this component can be subtracted from the shear load transferred by the

concrete.

Given the increasing use of finite element methods (FEA) in research with structural elements, more studies are needed for the correct understanding involving the punching effect with the use of prestressed concrete in flat slabs. According to Milligan et al. [12], FEA is an effective way to predict the capacity, failure mode, crack patterns and general behavior of concrete structures. From experimental test data, it is possible to obtain a calibrated numerical model, and thus, a parametric study can complement the experimental databases to have a better understanding of the structural behavior of flat concrete slabs.

Therefore, the objective of this work is to study the behavior of unbonded post-tensioned concrete flat slabs subjected to punching shear by means of nonlinear numerical analyses. This study investigated, from calibrated models in the ATENA finite element software, the interference caused by the layout of the prestressing cables varying their spacing and eccentricity. The values of failure loads, displacements, strains and crack propagation were also compared between the models, and thus it was observed how much the eccentricity of the cables interferes with the punching shear resistance.

## 2 Simulation of numerical models

Numerical analyses and investigations in this work were performed through calibration. A parametric study based on the constitutive model was implemented in the ATENA 3D software [13], which combined the behavior of traction (fracture) and compression (plastic). The constitutive models adopted are in accordance with Brigo et al. [3], Červenka and Červenka [13] and Brigo [14].

The models for calibration were based on experimental tests of flat slabs carried out in the study by Melges [1]. From this study, two models without transverse reinforcement were used, the M1 slab in reinforced concrete, and the M4 unbonded post-tensioned concrete flat slab. All slabs had dimensions of  $2500 \times 2500$  mm<sup>2</sup> and thickness of 160 mm, both supported by a steel plate in its central region of  $180\text{mm} \times 180\text{mm} \times 120\text{mm}$ , simulating the column. A set of metallic I-beams on the upper face of the slab prevented its movement while the upward load was applied incrementally by a hydraulic jack below the central steel plate, where reactions were measured by a load cell located between the hydraulic jack and the plate.

In the first step of numerical modeling, a study was carried out with the M1 model of Melges [1]. This first modeling aimed to determine the type of element, the discretization and the parameters of the constitutive model that best represent the results in adequate time. All stages and results of parameterization of the M1 model follow as described in Brigo [14]. The results for slab M1 showed a relationship between the numerical and experimental model at failure for load ( $V_{FEA}/V_{Exp}$ ) of 1.002 and displacement ( $D_{FEA}/D_{Exp}$ ) of 1.111.

For the prestressed slab model, M4, the same characteristics of dimensions and loading scheme as for slab M1 were maintained. The material properties are presented in Tab. 1. In this table,  $\varnothing_p$  is the equivalent diameter of a prestressing tendon,  $A_p$  is the cable area;  $V_p$  is the vertical component of the prestressing force acting on a critical section;  $E_p$  is the modulus of elasticity of the cables.

Table 1. Mechanical properties of materials, model M4 [1]

Concrete Properties			Prestressing Tendon Properties				Steel Properties			
$f_c$ (MPa)	$f_{ct}$ (MPa)	$E_c$ (MPa)	$\varnothing_p$ (mm)	$A_p$ (mm <sup>2</sup> )	$V_p$ (1%) (kN)	$E_p$ (MPa)	$\varnothing_s$ (mm)	$f_{sy}$ (MPa)	$f_{sr}$ (MPa)	$E_s$ (MPa)
51.92	3.87	30.46	12.7	99.9	182	208000	12.5	651.4	792.3	201541
							8	601.8	711.9	206900

As superior passive reinforcement, a mesh of 12.5 mm bars was used every 100 mm and an average usable height of 12.8 mm. As inferior passive reinforcement, in turn, a mesh with bars of 8 mm every 100 mm was adopted. As prestressing, 16 CP-190 RB 7 unbonded post-tensioned were used. The numerical model used is represented in Fig. 1a, and in Fig. 1b the geometric characteristics referring to prestressing are presented.

The forces applied to the strands are in accordance with Table 2 and refer to the re-stressing of the tendons in the experimental model. To better represent the experimental test process, the numerical model was divided into three loading intervals, namely; application of incremental displacement on the column until the slab reaches a reaction of 80 kN, application of standard forces according to Tab. 1, and in the third step, master-slave node connections are activated between the end of the cable and the highest node close to the anchor plate followed by the application of an incremental displacement in the column until the slab reaches failure.

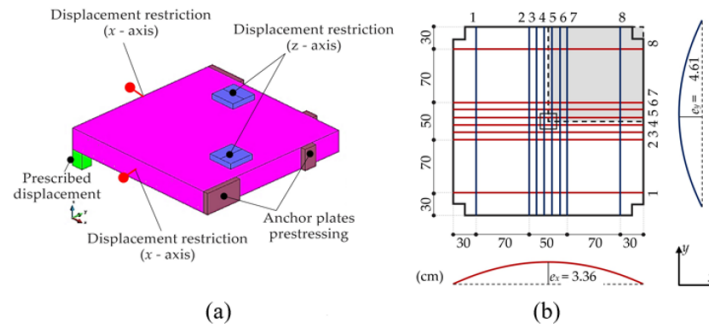


Figure 1. Numerical model M4 and boundary conditions (a), Characteristics of the experimental model (b)

Table 2. Prestressing force on tendons (kN) [1]

	Direction x				Direction y			
	5	6	7	8	5	6	7	8
Re-stress	128.77	129.61	133.21	130.61	128.65	132.29	127.48	131.94

Comparisons of numerical results with the experimental model were based on load-displacement and load-strain curves. In the curves of Fig. 2a, it is possible to observe the moment of application of prestressing along the crescent line without displacement variations, justified by the prestressing applied simultaneously to all cables. At the end of prestressing, the numerical model reached 218.74 kN compared to 221.30 kN for the experimental model. The numerical response managed to reproduce the test curve with good precision, with a  $V_{FEA}/V_{Exp}$  of 1.016, and  $D_{FEA}/D_{Exp}$  of 1.063, values that are sufficiently accurate. Good convergence was also found for concrete strain at position E25, as shown in Fig. 2b, with a small discrepancy only in the initial phase, when prestressing is applied. Figure 2c shows the strain of a tensioned bar, position E6, and in Fig. 2d a compressed bar, E18. Both numerical curves managed to capture the trend of the experimental curve.

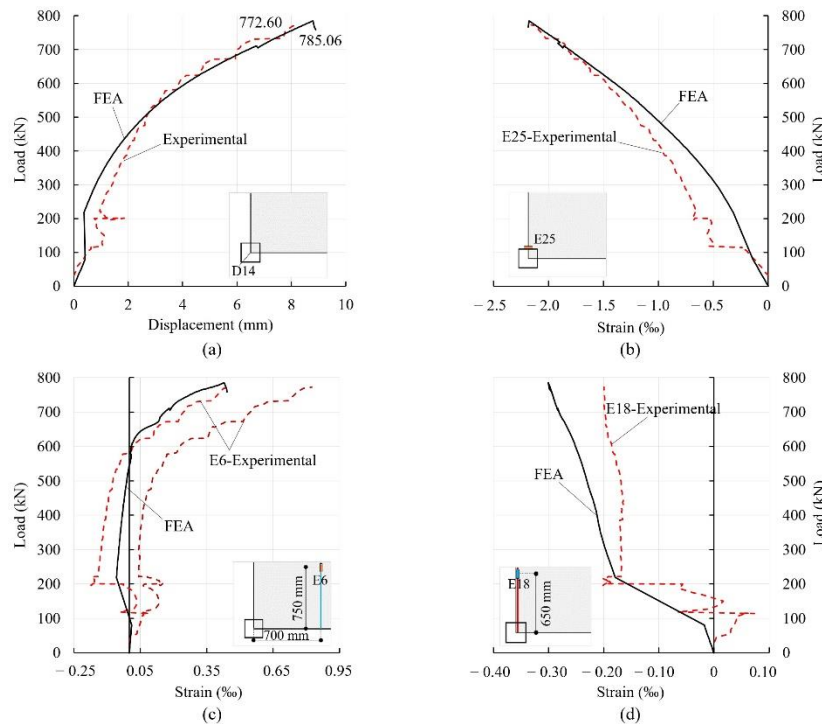


Figure 2. Comparison of numerical and experimental results of model M4, Load-displacement (a), Load-strain of concrete (b), Load-strain in tension bar (c), Load-strain in compressed bar (d)

### 3 Parametric study

In order to identify the influence exerted by the layout of the prestressing tendons on the punching shear resistance, a parametric study was carried out varying the spacing between the central tendons of the slab and their eccentricities. Therefore, the new models maintained the same characteristics according to the calibration of the M4 model, that is, geometry, materials, longitudinal reinforcement rate, characteristics of the prestressing cables and the force applied to them, as well as boundary conditions and monitoring points. Only the analyzed parameter varied.

Two series were evaluated, with the models of Series A maintaining the eccentricity with parabolic curvature of the cables, as shown in Fig. 1b. In the EC Series models, the prestressing cables were made straight, without curvature and eccentricity in the geometric center of the slab. The models of the two series were made with variations in the spacing between the prestressing cables in the central region of the slab, as shown in Fig. 3, with variations of 5 cm, 10 cm, 15 cm and 20 cm, defined by the nomenclature series-spacing. Thus, the Series A model with a spacing of 5 cm is represented as A-5 and the Series EC as EC-5.

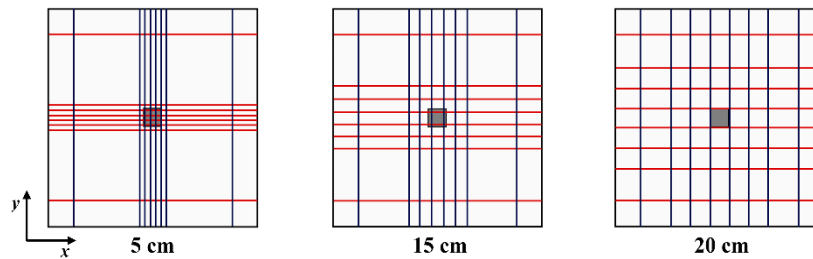


Figure 3. Spacing in plan of the prestressing cables

#### 3.1 Comparison between Series A and EC Results

With the results achieved with the two series, it was possible to evaluate the degree of interference caused by spacing and eccentricity in the pretension tendons. Table 3 shows the maximum load ( $V$ ) obtained for each model of the two analyzed series.

Table 3. Maximum capacity of each A and EC Series model

Series A	$V$ (kN)	Series EC	$V$ (kN)
A-5	788.12	EC-5	655.06
A-10	785.06	EC-10	619.18
A-15	753.17	EC-15	638.85
A-20	690.83	EC-20	600.96

Fig. 4a presents the load-displacement curves of the four slab models, as well as the experimental model. It was observed that, by increasing the spacing between the cables, there is a reduction in punching shear capacity. In addition, it is possible to notice that the A-5 model presented an increase in resistance, which is justified by the fact that the surface of the slab with the column coincided with two prestressing cables.

With the EC Series, it is possible to assess the degree of interference caused by the eccentricity of the prestressing tendons. The experimental curve was maintained for the purpose of comparing the load-displacement curves of the four slab models. In Fig. 4b, the load-displacement results show a significant reduction in punching shear resistance when keeping the prestressing cables straight without eccentricity. Another relevant aspect is observed at the end of prestressing application. The Series A models showed resistance gains greater than 130 kN; on the other hand, the Series EC models had an influence of only 20 kN, which demonstrates the strong influence caused by the eccentricity of the tendons.

As with the Series A models, increasing the spacing between the prestressing cables also resulted in a decrease in the resistance of the models. However, it can be seen that this reduction was less significant, at only 9% between the EC-5 and EC-20 models, compared to 14% between the A-5 and A-20 models.

Regarding the strain of the concrete, in all eight models it revealed a very similar behavior between the curves, with only a difference in the moment close to the failure. There is also greater stability of concrete when

centered prestressing is applied. In addition to reducing the resistance, it is possible to notice in Fig. 5a and 5b that the increase in the spacing between the cables caused a reduction in the ability to withstand strains. In models with greater spacing, a reduction in the maximum strain is observed, indicating a more fragile rupture, justified by the anticipation of the rupture of the models.

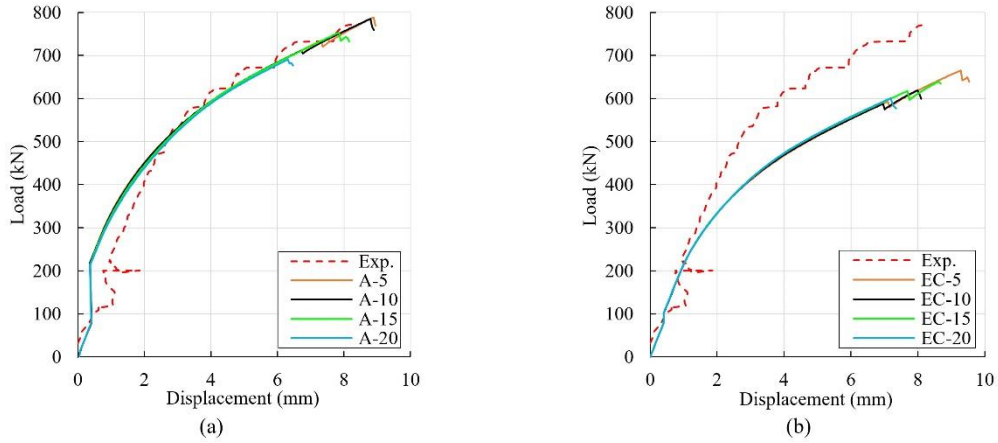


Figure 4. Load-displacement curves, Series A (a), Series EC (b)

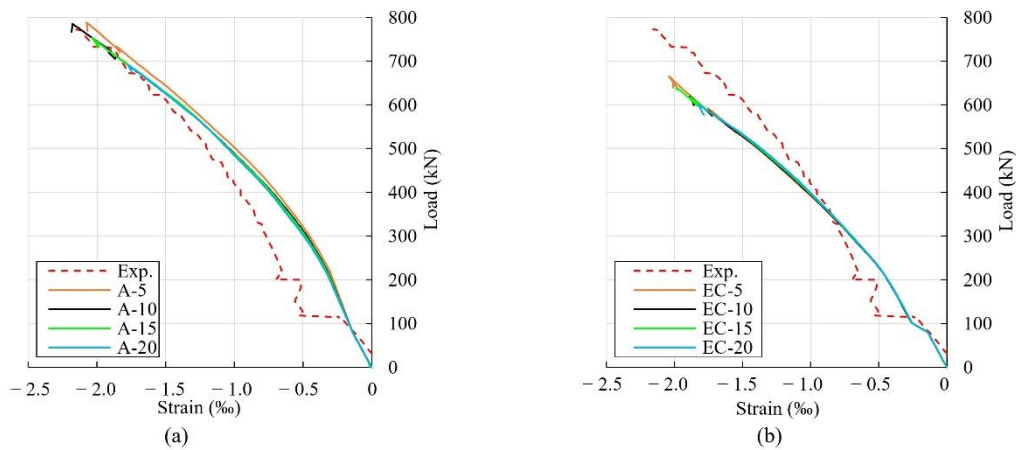


Figure 5. Concrete load-strain curves, Series A (a), Series EC (b)

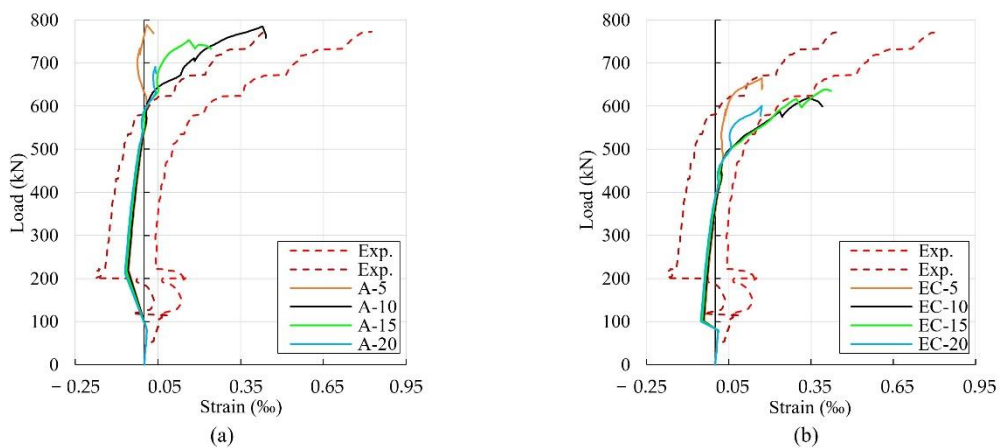


Figure 6. Tensile steel load-strain curves, Series A (a), Series EC (b)

By analyzing the curves of the eight load-strain models, in both series, in steel in tension (Fig. 6a and 6b), it is possible to notice a similar behavior up to a value close to 600 kN, which, in turn, does not demonstrate interferences in steel by changing the eccentricity of the tendons. This behavior can also be explained by the values close to the yield stress of the bars. From this point onwards, the strain of the models differs, with the A-5 and EC-5 models showing greater stability in strains. In the lower compressed bars (Fig. 6c and 6d), a good convergence of the results is observed, as well as the degree of interference caused by the spacing between the prestressing cables.

## 4 Conclusions

The results of the numerical analyses showed strong correspondence with the experimental data, so that the models were able to correctly predict punching failure in concrete slabs. In view of the good convergence of results, a parametric study of new structural models was presented.

The numerical models presented for Series A allowed the evaluation of the influence that the spacing between the prestressing cables exerts on the shear strength. In the analyzed models, there was a reduction in the resistance to punching shear and strain of the concrete.

For the models of the EC Series, they were evaluated regarding the interference caused by the increase of eccentricity in prestressing cables. Based on the models presented, it is possible to conclude that the eccentricity of the cables exerts a great influence on the punching shear resistance.

**Acknowledgements.** This research was financed in part by the Coordenação de Aperfeiçoamento de Pessoal de Nível Superior-Brasil (CAPES)-Finance Code 001.

**Authorship statement.** The authors hereby confirm that they are the sole liable persons responsible for the authorship of this work, and that all material that has been herein included as part of the present paper is either the property (and authorship) of the authors, or has the permission of the owners to be included here.

## References

- [1] J. L. P. Melges, *Análise experimental da punção em lajes de concreto armado e protendido*. PhD thesis, University of São Paulo, 2001.
- [2] F. J. Vecchio, P. Gauvrea, K. Liu, "Modeling of unbonded post-tensioned concrete beams critical in shear". *ACI Struct J.* 2006, 103(1), 57–64.
- [3] H. Brigo, L. J. Ashihara, M. G. Marques, E. A. P. Liberati, "Non-Linear analysis of flat slabs prestressed with unbonded tendons submitted to punching shear". *Buildings*, v. 13, p. 1-23, 2023.
- [4] H. Nylander, S. Kinnunen, H. Ingvarsson, "Punching of a prestressed and normally reinforced concrete bridge slab supported by a column". *Technical Report*; 1977.
- [5] J. Pralong, W. Brändli, B. Thürlimann, *Durchstanzversuche an stahlbetonund spannbetonplatten*. 7305. Birkhäuser; 1979
- [6] I. Shehata, *Punching of prestressed and non-prestressed reinforced concrete flat slabs*. PhD thesis. London, England: Polytechnic of Central London; 1982.
- [7] G. Corrêa, *Puncionamento em lajes cogumelo protendidas com cabos não aderentes*. Master thesis. Brasília, Brazil: University of Brasília, 2001.
- [8] A. P. Ramos, V. J. Lúcio, P. E. Regan, "Punching of flat slabs with in-plane forces". *Eng Struct.* 2011; 33(3): pp. 894–902.
- [9] T. A. P. Clément, M. F. Ruiz, A. Muttoni, "Influence of prestressing on the punching strength of post-tensioned slabs". *Eng. Struct.* 2014, 72, 56–69.
- [10] R. A. Diaz, L. M. Trautwein, T. N. Bittencourt, "Numerical investigation of the punching shear capacity of unbonded post-tensioned concrete flat slabs". *Structural Concrete*, 2020, 22, pp. 1205-1222.
- [11] A. A. El-Sisi, A. I. Hassanin, H. F. Shabaan, A. I. Elsheikh, "Effect of external post-tensioning on steel–concrete composite beams with partial connection". *Eng. Struct.* 2021, 247, 1–15.
- [12] G. J. Milligan, M. A. Polak and C. Zurell, "Finite element analysis of punching shear behaviour of concrete slabs supported on rectangular columns". *Engineering Structures*, vol. 224, 2020.
- [13] V. Červenka, L. Jendele, J. Červenka, *J. ATENA Program Documentation Part 1 Theory*; Červenka Consulting s.r.o.: Prague, Czech Republic, 2016, p. 282.
- [14] H. Brigo, *Análise não linear de lajes lisas protendidas com cabos não aderentes submetidas à punção*. Master thesis, State University of Maringá, 2023.